

Nonlinear finite element analysis of prestressed concrete box section beams

Ihsan A. S. Al-Shaarbaf

Hiba Emad Abbas

Civil Engineering Department, College of Engineering, Alnahrain University

Abstract:

This study presents a three-dimensional nonlinear finite element model suitable for the analysis of prestressed concrete box beams up to failure. Concrete was modeled using three-dimensional 20-node isoparametric quadratic brick elements, while the prestressing and reinforcing bars were modeled as one dimensional axial members embedded within the concrete elements. The behavior of concrete in compression is simulated using an elasto-plastic work hardening model followed by a perfectly plastic response, which is terminated at the onset of crushing. In tension, a smeared crack model with orthogonal cracks has been used with the inclusion of a model for the retained post-cracking tensile stresses and a model that reduces the shear modulus of rigidity after cracking. The nonlinear equations of equilibrium have been solved using an incremental-iterative technique based on the modified Newton-Raphson methods. The numerical integrations have been carried out using the 27-Gaussian-quadrature integration rule. Different types of prestressed concrete beams have been analyzed, and the finite element solutions are compared with the available experimental data. The finite element results obtained were the load-deflection response. Several parametric studies have been carried out to investigate the effects of some important finite

element and material parameters on the behavior of prestressed concrete box section beams. In general, good agreement between the finite element solutions and the available experimental results has been obtained. A study was made to compare the finite element ultimate moment of prestressed concrete box beams obtained for different values of compressive strength of concrete and area of prestressing steel with the provisions of the ACI-Code (318M-05). It was found that the predicted values of the ultimate moments obtained using the finite element analysis are in good agreement with the corresponding values obtained using the provisions of the ACI-Code (318M-05).

Keywords: Box Beams, prestressed Concrete, Finite Element.

Introduction

Box beams are referred to as thin-walled structures because of their cross-sectional dimensions. Box beams have been used extensively in bridge construction, because of the structural advantages of closed box section. The closed box section has a high torsional stiffness, which ensures good transverse distribution of eccentric loads. As the box section has a high bending stiffness, this leads to efficient use of the complete cross-section [1]. Box beam cross-

sections may take the form of single cell (one box), multi-spine (separate boxes), or multi-cell with a common bottom flange (contiguous boxes or cellular shape) [2]. The main objective of this research work is to investigate the overall structural behavior of prestressed concrete box beams using finite element models by using a modified computer program [3DNFEA] which was originally developed by Al-Shaarbaf [3] and modified by Tawfieq [4].

FINITE ELEMENT FORMULATION

The three-dimensional model is adopted in the present study. The 20-node hexahedral isoparametric elements are used as shown in Fig. (1) [5].

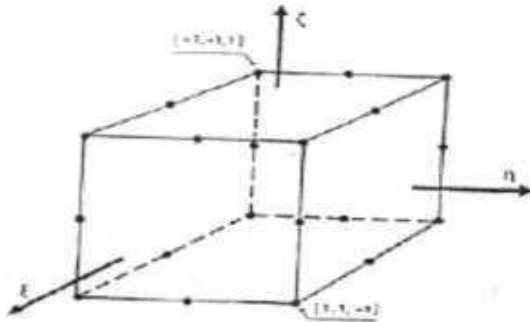


Figure (1) The 20-node isoparametric brick element [5].

Both prestressed and reinforcing bars are represented in this work as onedimensional axial members embedded within the brick elements. Perfect bond between the steel bars and the surrounding concrete is assumed to occur [6]. Full details on both theory and performance of the brick element are given in references [3, 4, 7].

MODELING OF MATERIAL PROPERTIES

Modeling of Concrete

The behavior of concrete in compression is simulated by an elasto-plastic work hardening model followed by a perfectly plastic response, which is terminated at the onset of crushing as shown in Fig. (2). the model used for compression is expressed in terms of yield criterion, a hardening rule, a flow rule and a crushing condition [8].

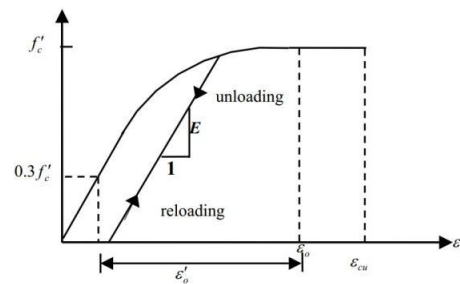


Figure (2) Uniaxial stress-strain curve for concrete adopted in the analysis [3].

Linear elastic model prior to cracking is usually used to simulate the behavior of concrete in tension [3]. In the present research, the onset of cracking is controlled

By a maximum principal stress criterion. A smeared crack model with fixed orthogonal cracks is adopted to represent the fractured concrete. The adopted model is described in terms of cracking criterion, formulation and shear retention model. Tension-stiffening parameters shown in Fig. (3) and shear retention model as shown in Fig. (4). Details of the modeling of material properties can found in references [3, 4, 7].

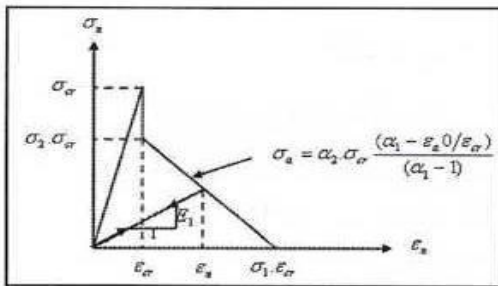


Figure (3) Tension-stiffening model for concrete [3].

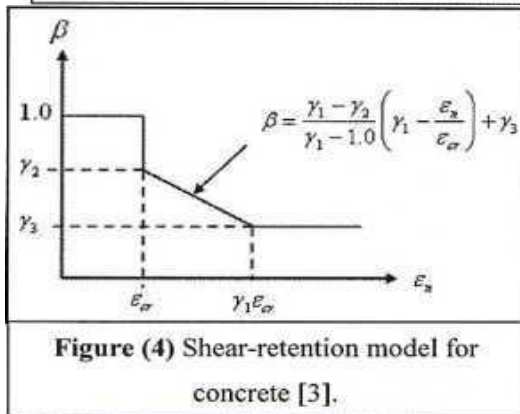


Figure (4) Shear-retention model for concrete [3].

Modeling of Reinforcement

The stress-strain behavior of reinforcement is assumed to be identical in tension and compression. The steel bars are long and relatively slender, and therefore, they can be assumed to transmit axial force only [3]. In the current work, an elastic linear work hardening model is adopted to simulate the niaxial stress-strain behavior of prestressing steel and reinforcing bars, Fig. (5).

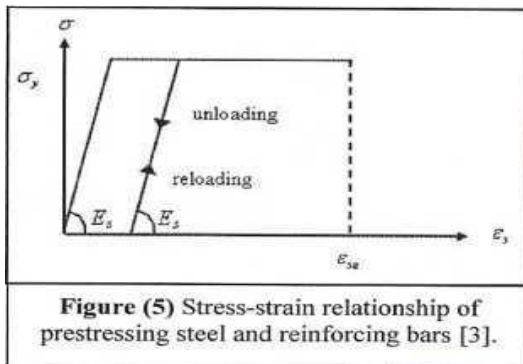


Figure (5) Stress-strain relationship of prestressing steel and reinforcing bars [3].

MODEL VERIFICATION

The adopted nonlinear finite element model is used to investigate the behavior of prestressed concrete box beams. Two examples are considered, these examples are ordinary reinforced concrete box beam and prestressed concrete box beam. The finite element analyses have been carried out using the 27-point integration rule, with a convergence tolerance of 5%. The tension stiffening parameters were $\alpha_1=10$ and $\alpha_2=0.6$, while the adopted shear retention parameters were $\gamma_1=10$, $\gamma_2=0.5$ and $\gamma_3=0.1$. The modified Newton- Raphson method in which the stiffness matrix is updated at the 2nd, 12th, 22nd,.. , etc. iterations of each increment of loading has been adopted as nonlinear solution algorithm. The external applied load was modeled as nodal forces applied on the top surface along the thickness of the vertical wall.

Box Beam under Unsymmetrical Load

This member is an ordinary reinforced concrete simply supported. box beam subjected to unsymmetrical load. This test was presented by Lars and Graham [9]. This beam was previously analyzed by Al-Daoud [10] using thin — walled curved box beam element with eight degrees of freedom at each node. The beam was chosen for present research work in order to test the ability of the finite element model in predicting the behavior of reinforced concrete box beams. The beam is denoted as (TH-II-CI). Details of the geometry, reinforcement distribution and loading arrangement are shown in Fig. (6). during the experimental test, the deflection was

recorded at a distance (100mm) from the mid span.

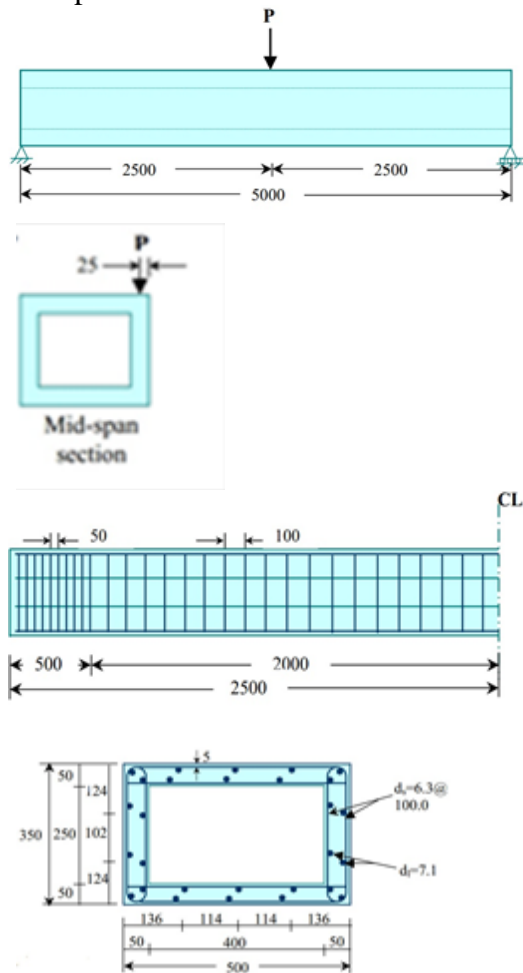
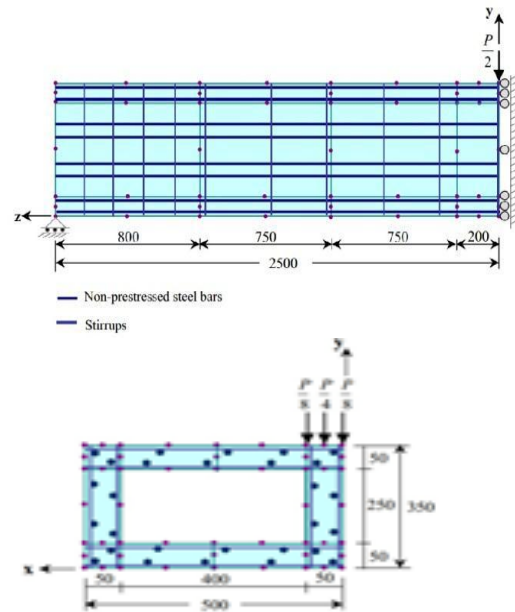


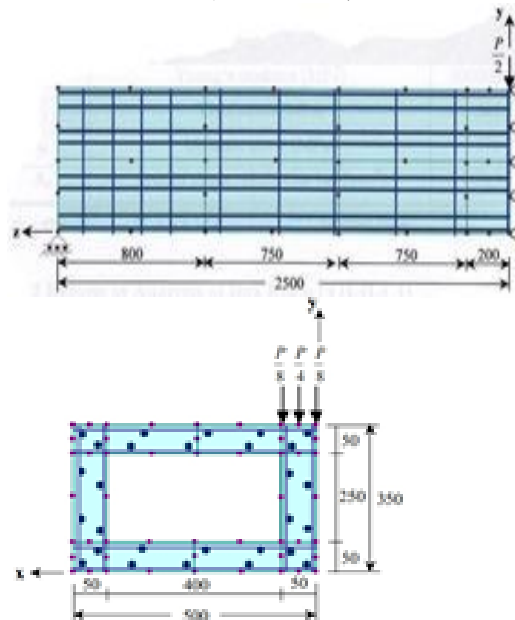
Figure (6) Dimensions and reinforcement details of box beam (TH-II-C1) [9].

By taking advantage of symmetry, only one-half of the beam has been used in the finite element analysis. The considered half of the beam was modeled using two different types of finite element mesh through the cross-section of the beam to show the effect of mesh type. The first type (mesh-A) had 40-quadratic brick elements. The adopted boundary and symmetry conditions are shown in Fig. (7a). The second type (mesh-B) consisted of 32- quadratic

brick elements. Boundary and symmetry conditions and loading arrangement for this mesh are shown in Fig. (7b). Material properties and the additional material parameters used for the two types of finite element mesh are listed in Table (1).



(a) Mesh-A, finite element idealization, symmetry and boundary conditions used for beam (TH-II-C1).



(b)Mesh-B, finite element idealization, symmetry and boundary conditions used for beam (TH-II-C1).

Figure (7) Finite Element meshes used for beam (TH-II-C1) [7].

Table (1) Material properties and material parameters used for beam (TH-II-C1).

Concrete		
E_c	Young's modulus (MPa)	33200*
f_c'	Compressive strength (MPa)	50.0
f_t	Tensile strength (MPa)	3.5**
ν	Poisson's ratio	0.2***
Non-prestressed steel bars		
E_s	Young's modulus (MPa)	200000***
f_y	Yield stress (MPa)	541
f_u	Ultimate stress (MPa)	590
A_s	Area of single reinforcing bar (mm ²)	38.3

* $E_c = 4700 \sqrt{f_c'}$, ** $f_t = 0.5 \sqrt{f_c'}$, *** Assumed value

The numerical load-deflection curves (at 100mm from mid span) obtained from this beam for two types of finite element meshes with Al-Daoud [10] results are compared with the experimental results (at 100mm from mid span) in Figs. (8) and (9). The figures reveal acceptable agreement between the finite element solutions and the experimental results throughout the entire range of loading. However the numerical behavior obtained using mesh type (B) is slightly better than that obtained using mesh type (A) as compared to the experimental response. Therefore mesh type (B) has been adopted in the following example.

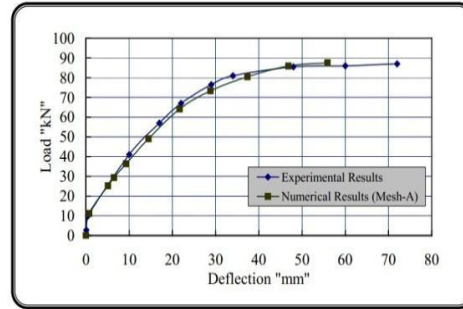


Figure (8) Experimental and numerical (Mesh-A) load-deflection behavior of box beam (TH-II-C1).

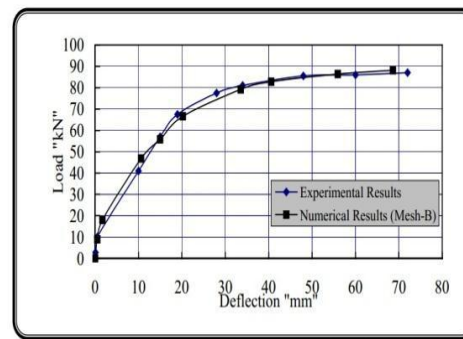


Figure (9) Experimental and numerical (Mesh-B) load-deflection behavior of box beam (TH-II-C1).

Prestressed Concrete Box Beam

The ordinary reinforced box section simply supported beam, which was tested by Lars and Graham [9] and is analyzed in section 4.1, was reanalyzed here again with the addition of three prestressing strands located at the bottom flange of the cross-section to investigate the accuracy and applicability of the adopted finite element model to predict the behavior of prestressed concrete box beams. This assumed beam is designated as (TH-II-C1-P). The beam was reinforced with ordinary longitudinal bars and three prestressing strands located as shown in Fig. 10. The prestressing strands had a total area of 75mm² and the effective prestressing stress of (1180MPa). The

geometry, reinforcement distribution and loading arrangement are, shown in Fig. (6). The beam cross-section is shown in Fig. (10).

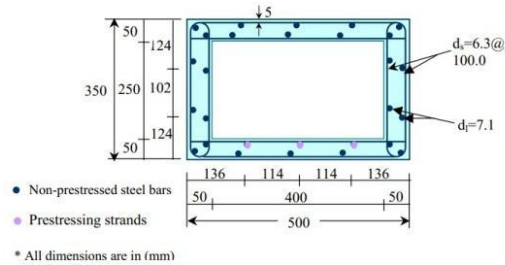


Figure (10) Dimensions and reinforcement details of the cross-section of prestressed concrete box beam (TH-II-C1-P).

By taking into consideration the advantage of geometric symmetry, a segment, representing one-half of the beam has been used in the finite element analysis. The considered segment was modeled using 32-hexahedral brick elements. The longitudinal prestressing and non-prestressing bars were modeled as one-dimensional elements embedded into the concrete elements. Before applying external load the prestressing effect was simulated by initial prestressing stress and strain at the sampling points representing the prestressing strands. The finite element mesh, together with the boundary and symmetry conditions and loading arrangement used are shown in Fig (7b). The cross-section mesh is shown in the Fig. (11). Material properties and the additional material parameters adopted in the analysis are shown in Table (2).

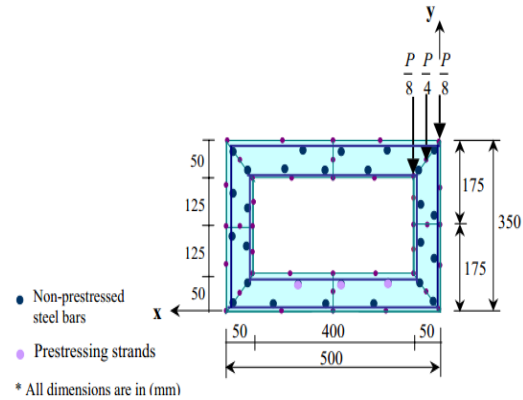


Figure (11). Finite element mesh, of cross-section used for prestressed box beam (TH-II-C1-P).

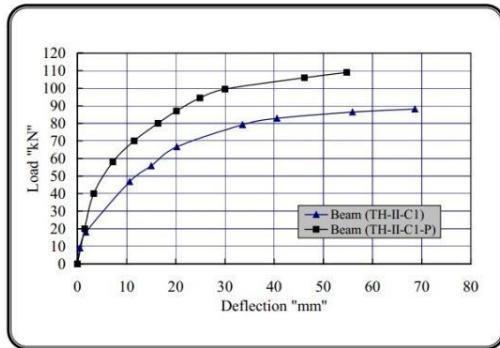
Table (2) Material properties and material parameters used for prestressed box beam(TH-II- CI-P).

Concrete		
E_c	Young's modulus (MPa)	33200*
f_c'	Compressive strength (MPa)	50.0
f_t	Tensile strength (MPa)	3.5**
ν	Poisson's ratio	0.2***
Non-prestressed steel bars		
E_s	Young's modulus (MPa)	200000***
f_y	Yield stress (MPa)	541
f_u	Ultimate stress (MPa)	590
A_s	Area of single reinforcing bar (mm ²)	38.3
Prestressing reinforcement		
E_s	Young's modulus (MPa)	200000***
f_{py}	Yield stress (MPa)	1822
f_{pu}	Ultimate stress (MPa)	1962
f_{ie}	Effective Prestressing stress (MPa)	1180
A_s	Area of prestressing strands (mm ²)	75

* $E_c = 4700 \sqrt{f_c'}$, ** $f_t = 0.5 \sqrt{f_c'}$, *** Assumed value

The numerical results obtained from the assumed prestressed concrete box beam (TH-II-C1-P) are compared with the numerical results obtained for non-prestressed concrete box beam (TH-II-CI). The finite element load-deflection curves drawn at a distance (100mm) from the mid span are shown in Fig. (12). A significant increase in the beam stiffness can be noticed for the prestressed beam as compared to the non-prestressed beam. The failure load

of the non-prestressed concrete box beam (TH-II-C1) is (88.19 kN), while the failure load of prestressed concrete box beam (TH-II-C1-P) is (109 kN). The ratio of the failure load of the prestressed beam to the non-prestressed beam is (1.24).



Numerical load-deflection behavior of box beams (TH-II-C1) and (TH-II-C1-P).

PARAMETRIC STUDY

In order to investigate the effects of some material and solution parameters on the behavior of prestressed concrete box beams, the members designated as (TH-II-C1) and (TH-II-C1-P) have been chosen to carry out the parametric study.

Effect of Concrete Compressive Strength (f_c)

Figs. (13) and (14) show the effect of using different values of grade of concrete on the predicted load-deflection response of box beams (TH-II-C1) and (TH-II-C1-P). In this study the selected values of the compressive strength of concrete (f_c) were 50, 60, 70, 80, and 90MPa for the beams (TH-II-C1) and (TH-II-C1-P). It can be noted from the figures that a stiffer response has been obtained for higher concrete compressive strength relative to normal concrete strength. This is because the mode of failure is primarily flexural type. Numerical ultimate loads obtained

for different values of grade of concrete of all tested members together with the deflection at ultimate loads are listed in Table (3).

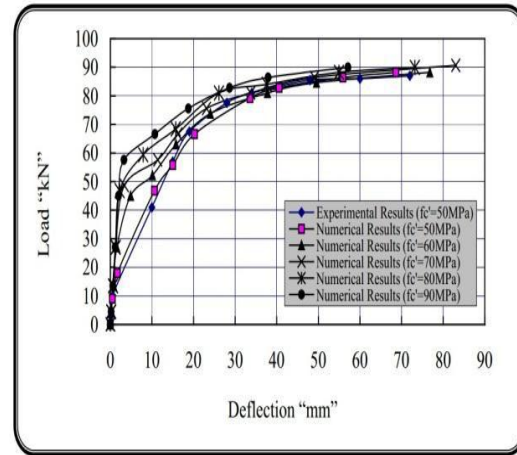


Figure (13) Effect of concrete compressive strength (f_c) on the load-deflection behavior of box beam (TH-II-C1).

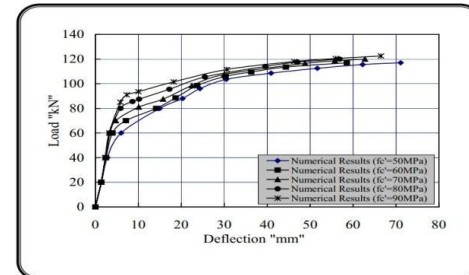


Figure (14) Effect of concrete compressive strength (f_c) on the load-deflection behavior of box beam (TH-II-C1-P).

Table (3) Effect of grade of concrete (f_c) on the predicted ultimate loads of box beams (TH-II-C1) and (TH-II-C1-P)

Value of (f_c)MPa	Numerical ultimate load (kN)	Deflection (mm) at ultimate load	$P_{N_{num.}}/P_{N_{Exp.}}$	
(TH-II-C1)	50	88.19	68.63	1.01**
(TH-II-C1)	60	88.19	76.79	1.01**
(TH-II-C1)	70	90.70	83.01	1.04**
(TH-II-C1)	80	89.99	73.19	1.03**
(TH-II-C1)	90	89.99	57.13	1.03**
(TH-II-C1-P)	50	117.00	71.10	-
(TH-II-C1-P)	60	117.00	58.54	-
(TH-II-C1-P)	70	120.00	62.76	-
(TH-II-C1-P)	80	120.00	56.88	-
(TH-II-C1-P)	90	122.50	66.49	-

* $P_{N_{Exp}}=54kN$ and $f_c_{Exp}=65MPa$ ** $P_{N_{Exp}}=87kN$ and $f_c_{Exp}=50MPa$

Table (4) Effect of amount of prestressing steel (Aps) on Beam the predicted ultimate load

Value of (A_{ps}) mm ²	Numerical ultimate load (kN)	Deflection (mm) at ultimate load	$P_{N_{num.}}/P_{N_{Exp.}}$	
(TH-II-C1-P)	45	103.00	74.20	-
(TH-II-C1-P)	75	117.00	71.10	-
(TH-II-C1-P)	105	117.00	31.35	-
(TH-II-C1-P)	135	120.00	25.60	-

* $P_{N_{Exp}}=54kN$, $f_c_{Exp}=65MPa$ and $A_{ps_{Exp}}=343\text{ mm}^2$

Effect of prestressing Steel (Aps)

In order to study the effect of amount of prestressing steel (Aps) on the behavior and ultimate load capacity of prestressed concrete box beam (TH-II-C1-P), different amounts of prestressing steel were used for the numerical analyses. These amounts were 45, 75, 105, and 135mm². Fig. (15) reveals the difference in the behavior response along the load-deflection curve. The figures indicate that as the amount of prestressing steel increases the ultimate load would also increase and the load-deflection curve would be stiffer than the load deflection curve obtained for less amount of prestressing steel. When the amount of (Aps) is increased from 45 to 135 mm², the ultimate load of prestressed concrete box beam (TH-II-C1-P) is increased by about 15%. The predicted ultimate load values and the deflection at ultimate load obtained from this study are listed in Table (4).

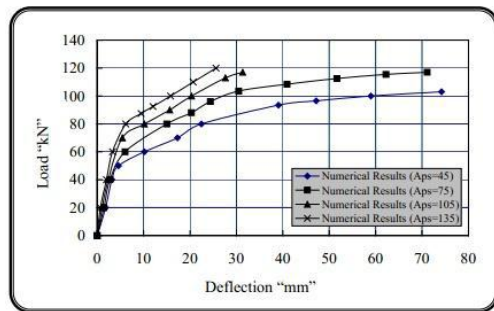
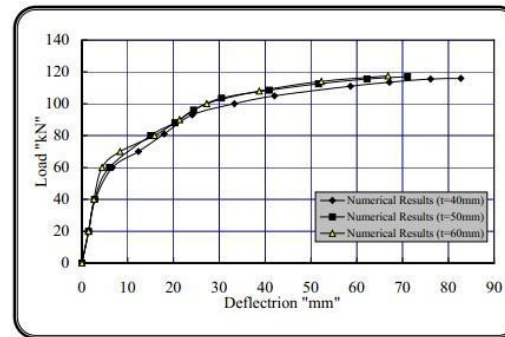


Figure (15) Effect of wall thickness of prestressed concrete

Effect of Wall Thickness of the Prestressed Concrete Box Beam

In order to study the effect of wall thickness of prestressed concrete box beam (TH-II-C1-P), the beam has been numerically analyzed using different values of wall thickness. The selected values were 40, 50 and 60mm. The results obtained from the finite element solutions represented by load-deflection curves are shown in Fig. [16]. It is obvious that the ultimate load increases as the wall thickness increases and load-deflection curve becomes stiffer. When the wall thickness is decreased from 50 to 40mm, the ultimate load is decreased by about 1.01%, while when the wall thickness is increased from 50 to 60mm the ultimate load is increased by about 1.004%. Values of predicted ultimate load and deflection at ultimate load for each value of wall thickness are listed in Table[5].



Figure(16) Effect of wall thickness of prestressed concrete box beam (TH-

II-C1-P) on the load deflection behavior.

Table (5) Effect of wall thickness on the predicted ultimate of prestressed concrete

Value of wall thickness (mm)	Numerical ultimate load (kN)	Deflection (mm) at ultimate load
(TH-II-C1-P) 40	116.00	82.73
(TH-II-C1-P) 50	117.00	71.10
(TH-II-C1-P) 60	117.50	66.81

Nominal Moment Capacity

Exact analysis for the nominal moment capacity of a prestressed concrete box section under flexure is a complicated theoretical problem because both steel and concrete are generally stressed beyond their elastic ranges. The method for determining the ultimate flexural capacity is detailed in reference [7].

Nominal Moment Capacity of Prestressed Concrete Box (TH-II-C1-P)

The method outlined in Ref. [7] has been adopted to compare the nominal moment capacity obtained using the ACI- Code provisions and results obtained using the finite element analysis. The prestressed concrete box beam (TH-II-C1-P) has been reanalyzed using different values of concrete compressive strength (f_c), and different amount of prestressing steel (Aps). The numerical nominal moment values obtained for the selected beam are compared in Table 6 with the ACI Code (318M-05) values for different concrete compressive strength. The selected values of concrete compressive strength were 40, 50, 60, 70, 80, and 90MPa, while the amount of prestressing steel and the effective prestressing steel stress were kept constant equal to 75 mm² and

1180MPa respectively. From this table it is shown that the nominal moment capacity obtained using the finite element method are in good agreement with the ACI Code (318M-05) values. The ratios of the numerical nominal moments to those calculated using the ACI Code provisions ranged between 1.0050 and 1.0754.

Table (6) ACI-Code and finite element nominal moments of prestressed concrete box beam (TH- II-C1-P) obtained for different values of concrete compressive strength.

f_c (MPa)	f_p (ACI) (MPa)	M_n (ACI) (kN.m)	M_n (F.E.A.) (kN.m)	$\frac{M_n (F.E.A.)}{M_n (ACI)}$
40	1943.28	92.02	92.50	1.0050
50	1945.72	92.57	95.00	1.0263
60	1946.74	92.93	96.88	1.0425
70	1948.71	93.21	98.13	1.0527
80	1950.19	93.43	98.75	1.0569
90	1951.34	93.57	100.62	1.0754

Table (7) summarizes the numerical and ACI Code nominal moment capacity of prestressed concrete box beam (TH-II-C1-P) obtained for different values of amount of prestressing steel and those obtained using ACI Code (318M-05) provisions. The selected values of prestressing steel area were 60, 75, 90, 105, and 135 mm², while the concrete compressive strength and the effective prestressing steel stress were kept constant equal to 50MPa and 1180MPa respectively. It can be noted that the predicted finite element nominal moments are in good agreement with those recommended by ACI Code (318M-05) provisions. The ratios of the numerical nominal moments to those calculated using the ACI Code provisions ranged between 1.0002 and 1.0263. It can be noted that as the amount of prestressing steel is increased,

the numerical nominal moment becomes close to the ACI-Code corresponding values.

Table (7) ACI-Code and finite element nominal moments of prestressed concrete box beam (TH- II-C1-P) obtained for different amounts of prestressing steel.

A_{ps} (mm ²)	f_{ps} (ACI) (MPa)	M_n (ACI) (kN.m)	M_n (F.E.A) (kN.m)	M_n (F.E.A) / M_n (ACI)
60	1948.70	83.52	85.62	1.0261
75	1945.72	92.57	95.00	1.0263
90	1942.76	101.56	103.75	1.0217
105	1941.13	110.52	111.87	1.0122
135	1933.88	128.11	128.13	1.0002

Conclusion

The conclusions drawn from work on prestressed concrete box beams based on the finite element analyses are:

1- The adopted three-dimensional nonlinear finite element model used simulates the behavior of prestressed concrete box beams under flexure. The numerical tests carried out for different case studies show that the predicted load-deflection behavior and the failure loads are in good agreement with the experimental results available.

2- When three strands having an area of 75mm and effective prestressing stress of 1180MPa were used for the ordinary reinforced concrete box beam (TH-II-C1) the numerical results reveal that an increase of about 25% in the ultimate load has been achieved.

3. The finite element solutions show that the value of concrete compressive strength can influence the post-cracking stiffness and the ultimate load value. The results reveal that an increase of 5% in the ultimate load has been achieved for prestressed concrete box beam (TH-II-C1-P), when the compressive strength of

concrete was increased from 50 to 90MPa.

4. It was found that for beam (TH-II- C1-P) an increase in the ultimate load of about 3% is gained when the area of prestressing steel increases from 75 to 135mm². Also the results reveal that a decrease of 12% in the ultimate load occurred, when the prestressing area was decreased from 75 to 45mm².

5. The finite element solutions of prestressed concrete box beam reveal that the ultimate load increases as the wall thickness of the box section is increased. When the wall thickness is increased from 50 to 60mm the ultimate load capacity is increased by about 0.5%. However, when the wall thickness is decreased from 50 to 40mm the ultimate load capacity is decreased by about 1%.

6. The nominal moment capacity of prestressed concrete box beams obtained using the finite element analysis is compared with that calculated using the ACI-Code (318M-05) provisions. This is achieved by taking different values of concrete compressive strength and different areas of prestressing reinforcement. It can be noted that the predicted numerical values are in good agreement with the values recommended by the ACI-Code provisions. The difference between the numerical and the ACI-Code results did not exceed (7%). This conclusion indicates that the ACI-Code equations are sufficiently reliable in predicting the moment capacity of prestressed concrete box beams with high values of concrete compressive strength.

References

1. Lars, J. R., "Plastic Behavior of Deformable Reinforced Concrete Box Sections under Eccentric Load" Ph.D.Thesis, Department of Civil Engineering, University of Queensland, 1996.
2. Khaled, M. S., and John, B. K., "State-of- the-Art in Design of Curved Box-Girder Bridges", Journal of Bridge Engineering, ASCE, Vol.6, No.3, May-June, 2001, pp. 159-167.
3. Al-Shaarbaf I. A. S., "Three-Dimensional Nonlinear Finite Element Analysis of Reinforced Concrete Beams in Torsion", Ph.D. Thesis, University of Bradford, 1990.
4. Tawfieq, A. M., "Nonlinear Finite Element Analysis of Prestressed Concrete Beams", M.Sc. Thesis, Al-Nahrain University, 2002.
5. Dawe, D. J., "Matrix and Finite Element Displacement Analysis of Structures", Clarendon Press, Oxford, U. K., 1984, 565 pp.
6. Chen, W. F., "Plasticity in Reinforced Concrete", McGraw-Hill, Book Company, New York, 1982,474 pp.
7. Chen, W. F., and Saleeb, A. F., "Constitutive Equations for Engineering Materials: Elasticity and Modeling", Vol. 1, John Wiley and Sons, New York, 1982.
- 8.Owen, D. R. J., and Hinton, E., "Finite Element in Plasticity: Theory and Practice", Pineridge Press, Swansea, U.K., 1980, 594 pp.
- 9.Lars, J. R., and Graham, B., "Large-Scale Experimental Investigation of Deformation RC Box Sections", Journal of Structural Engineering, ASCE, Vol. 125, No. 3, March, 1999, pp. 227-235.
- 10.Al-Daoud, W. Z., "Nonlinear Analysis of Curved Reinforced Concrete Rectangular Box Girder", Ph.D. Thesis, Al-Nahrain University, 2006.
- 11-Lin, T. Y., and Bums, H., "Design of Prestressed Concrete Structures", 3rd edition, John Wiley and Sons, New York, 1982,646 pp.
- 12- ACI Committee 318, "Building Code Requirements for Structure Concrete (ACI 318-05) and commentary (ACI 318R-05)", American Concrete Institute, Farmington Hills, MI, 2005,430 pp.
- 13- Abbas, H. E., "Nonlinear Analysis of Prestressed Concrete Box Section Beams", M.Sc. Thesis, Al-Nahrain University, 2007.

التحليل اللاخطي للعنصر المحدود من خلال تسليط الاشعة على الخرسانة مسبقة الاجهاد قبل وبعد التشقق

احسان علي صائب هبة عماد عباس

جامعة النهرين - كلية الهندسة - هندسة مدني

الخلاصة:

اعتمدت هذه الدراسة على استخدام العناصر المحددة ثلاثية الابعاد لاجراء التحليل اللاخطي وتحري سلوك العتبات الخرسانية مسبقة الاجهاد لمراحل التحليل قبل وبعد التشقق والى حد الحمل الاقصى. استخدام العنصر الطابوقي ذي العشرين عقدة لتمثيل الخرسانة، اما حديد التسليح بنوعية العادي والمسبق الاجهاد فقد تم تمثيله بعناصر محورية مطمورة داخل العنصر الطابوقي. تم تمثيل الخرسانة تحت تأثير اجهادات الضغط باستخدام النموذج المرن ذي التقوية الانفعالية (Hardening Elasto-Plastic Work) والمتبوع بتصرف تام اللدونة (Plastic Perfectly) يستمر لغاية تهشم الخرسانة (Concrete Crushing Of). اما بالنسبة لتصرف الخرسانة تحت تأثير اجهادات الشد فقد اعتمد نموذج الشق المنتشر (Model Smeared) لاحتساب اجهادات الشد المتبقية في الخرسانة المسلحة بعد التشقق. كما تم تبني انموذج احتباس اجهادات القص (Shear-Retention Model) والذي يقوم بتخفيض معامل صلابة القص (Shear Modulus Rigidity) المتبقي في مرحلة ما بعد التشقق. تم حل معادلات التوازن اللاخطية باستخدام طريقة تزايدية تكرارية (Incremental-Iterative Model) واستخدام في الحل الطريقة المعدلة لنيوتن-رافسن (Modified Newton Raphson Method) مع اجراء التكاملات العددية باستخدام طريقة التكامل ذات السبع والعشرين نقطة تكامل. تم تحليل انواع مختلفة من العتبات الخرسانية مسبقة الاجهاد وقورنت النتائج المستحصلة منحنيات الحمل-الازاحة (Load-Deflection) المستحصلة بطريقة العناصر المحددة مع النتائج المختبرية المتوفرة. أجريت بعض المتغيرات المهمة على سلوك العتبات الخرسانية مسبقة الاجهاد ذات المقاطع الصندوقية. بشكل عام فقد تم الحصول على توافق جيد بين النتائج التحليلية بطريقة العناصر المحددة والنتائج المختبرية. ان العزوم القصوى للعتبات الخرسانية ذات المقاطع الصندوقية المسبقة الاجهاد المحسوبة من علاقات مدونة الخرسانة الامريكية (ACI-Code 318M-05) قورنت مع النتائج المستحصلة من طريقة العناصر المحددة ولقيم مختلفة من مقاومة الانضغاط للخرسانة ومساحة حديد التسليح مسبق الاجهاد. لقد وجد انه ولقيم عالية من مقاومة الانضغاط للخرسانة لم يتجاوز الفرق بين العزوم المستحصلة بطريقة العناصر المحددة نسبة 7% عن مثيلاتها المستخرجة من معدلات مدونة الخرسانة الامريكية.